

where the factor involving $\partial\eta/\partial E$ plays essentially the same role here as the $(\langle P_2^0(\cos\theta) \rangle_j - \langle P_2^0(\cos\theta) \rangle)$ of Eqs. (11) and (19)–(23). We may rewrite this as

$$q_{10c}(T) - q_{10c}(0) = \sum_j \left\{ \Delta n(T)_j \langle 2r^{-3}P_2^0(\cos\theta) \rangle_j + \frac{\pi^2}{3} (kT)^2 \eta(E_F)_j \right. \\ \left. \times \left[\frac{\partial \langle 2r^{-3}P_2^0(\cos\theta) \rangle_j}{\partial E} \right]_{E_F} \right\} + O(T^4). \quad (\text{A6})$$

The first term of either Eq. (A5) or (A6) represents the thermal repopulation, $\Delta n(T)_j$, into or out of the j th Fermi-surface region and the second term represents the change in q_{10c} due to thermal repopulation normal to the Fermi surface. Despite superficial dissimilarities, these equations include the $q'(T) - q'(0)$ term of Eqs. (A3) and (A4). Standard assumptions were made in deriving these equations, namely that $\eta(E)_j$ and $\langle 2r^{-3}P_2^0(\cos\theta) \rangle_j$ vary slowly with respect to $\partial g(E)/\partial E$ in the energy range $E_F \pm kT$. Normally such requirements are reasonably well met in a metal but this may be marginal for the V_3X compounds. If so, not only are the above equations suspect for these compounds but

so are the existing analyses of the electronic specific heats and the temperature-dependent spin susceptibilities.

Estimates of $q_{10c}(T) - q_{10c}(0)$ are more formidable than any already made in this Appendix and elsewhere in this paper because we require knowledge of $\eta(E)_j$ and $\langle 2r^{-3}P_2^0(\cos\theta) \rangle_{j,E}$ as a function of both j and E (in the vicinity of E_F).

An effect which could decrease the expected temperature dependence of the field gradients is the self-consistency and associated saturation behavior discussed in Sec. IV. Limiting attention to direct Coulomb F^2 terms, one expects saturation to reduce the temperature dependence of $q_{10c}(T)$. This becomes obvious if the orbitals in the vicinity of the Fermi surface have essentially common radial character because any thermal j repopulation [the first line of Eqs. (36)–(37)] causing q_{10c} to change will then also produce a repopulation potential term [e.g., see Eqs. (14)–(20)] which opposes the repopulation. This is due to the common angular character of the gradient and the F^2 potential operators. Both experimentally and in the observations of the preceding sections, there is the suggestion that saturation effects play a significant role in the V_3X compounds.

Compressibility and Electrical Conductivity of Cadmium Sulfide at High Pressures

G. A. SAMARA* AND A. A. GIARDINI†

U. S. Army Electronics Laboratories, Fort Monmouth, New Jersey

(Received 7 May 1965)

The compressibility and electrical conductivity of CdS were investigated to over 60 kbar under nearly hydrostatic conditions. Volume change was measured by the inductive-coil technique. In single-crystal samples, the wurtzite \rightarrow rocksalt phase transformation starts at 23 ± 1 kbar at 25°C. At the transition a sudden volume change of 21% occurs, and the electrical resistivity decreases by several orders of magnitude. The average volume compressibilities are 18.2×10^{-4} kbar $^{-1}$ for the wurtzite phase (0–23 kbar) and 9.5×10^{-4} kbar $^{-1}$ for the rocksalt phase (40–60 kbar). Both phases exhibit semiconducting behavior. For the high-resistivity samples used ($\rho > 10^8 \Omega \text{ cm}$), an activation energy of 0.9 eV and a band gap of $\simeq 2.3$ eV were obtained for the wurtzite phase. Both increase with pressure. For the rocksalt phase an activation energy of 0.1–0.2 eV and a band gap of $\simeq 1.3$ eV were obtained. The progress of the forward and reverse transitions was followed visually under high magnification, and some observations are made concerning the mechanism of the transformation.

I. INTRODUCTION

CADMIUM sulfide (CdS) is a dimorphous compound crystallizing in both the hexagonal wurtzite and the related cubic zincblende structures. Both of these are loosely packed structures which transform to phases with closer packing at high pressure. Drickamer

and co-workers,^{1–3} using optical and electrical techniques, were the first to report a pressure-induced polymorphic transition in CdS. The transition, observed in the range 20–30 kbar, is accompanied by a large discontinuous red shift in the optical-absorption

* Present address: Sandia Laboratory, Albuquerque, New Mexico.

† Present address: Department of Geology, University of Georgia, Athens, Georgia.

¹ A. L. Edwards, T. E. Slykhouse, and H. G. Drickamer, *J. Phys. Chem. Solids* **11**, 140 (1959); A. L. Edwards and H. G. Drickamer, *Phys. Rev.* **122**, 1149 (1961).

² G. A. Samara and H. G. Drickamer, *J. Phys. Chem. Solids* **23**, 357 (1962).

³ S. Minomura, G. A. Samara, and H. G. Drickamer, *J. Appl. Phys.* **33**, 3196 (1962).

edge¹ and a corresponding increase by several orders of magnitude in the electrical conductivity.² In both of these investigations single-crystal samples in the wurtzite structure were used. Jayaraman *et al.*⁴ studied the compression of powdered samples using a piston-cylinder apparatus and reported a volume decrease of $\sim 10\%$ at the transition.

A number of authors have investigated the structure of the high-pressure phase of CdS using high-pressure x-ray cameras.⁵⁻⁸ It is agreed that the new phase has the cubic NaCl (rocksalt) structure, and that the overall volume decrease is $\sim 25\%$. This value includes the sudden volume change at the transition and the compression of the wurtzite phase. Upon releasing the pressure, the structure of the recovered material is mostly zincblende with some wurtzite.

In the present work we carried out an investigation of the compressibility (up to 60 kbar) and the electrical conductivity (up to 80 kbar) of CdS at room and elevated temperatures. Single-crystal and polycrystalline samples were used. Compressibility was studied using our recently developed inductive-coil technique.⁹ The availability of the x-ray data on CdS from three different sources offered us an excellent opportunity to check the accuracy of the coil method. The temperature dependence of the conductivity of both phases was studied over a wide temperature range and estimates of the widths of the energy gaps obtained. Progress of the forward and reverse transitions and the accompanying color changes were followed visually by means of a pressure cell of the type described by Van Valkenburg.¹⁰

II. EXPERIMENTAL TECHNIQUES

The pressure apparatus used for the compressibility work is a large cubic multianvil unit.¹¹ Pyrophyllite was used for specimen containers and served as the pressure transmitting medium. Standard containers (5.65 cm between opposite faces) with integral preformed gaskets were used throughout the investigation.¹¹ The large size of the sample chamber allowed us to use techniques whereby the sample experiences no measurable pressure gradients and very low residual deformation.^{9,12} CdS samples as large as 1.25 cm long

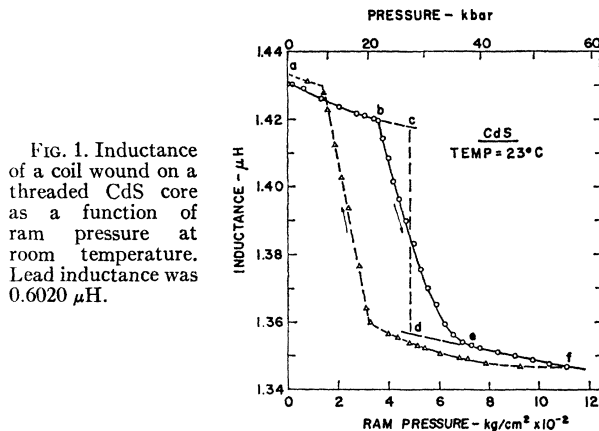


FIG. 1. Inductance of a coil wound on a threaded CdS core as a function of ram pressure at room temperature. Lead inductance was $0.6020 \mu\text{H}$.

$\times 0.90$ -cm diam were recovered with less than $\pm 3\%$ change in dimensions after compression to 60 kbar, with smaller samples showing considerably less change.

The change in sample volume with pressure was measured using the inductive coil technique⁹ along with some improvements.¹² Among these are the use of a high-pressure coaxial cable to replace the two parallel copper leads to the coil and the winding of the coil directly on a threaded sample.

The CdS samples for the volume measurements (wurtzite form) were cut from a large ingot. The material was doped with indium, but the indium concentration was small as evidenced by high sample resistivity ($\rho > 10^6 \Omega \text{ cm}$). Finished samples varied in size from 0.635 cm diam \times 0.635 cm long to 0.900 cm diam \times 1.25 cm long with from 16 to 28 threads/cm. Formvar-coated 0.010–0.014-cm diam copper wire was used for the coils.

For the room-temperature measurements, the sample with the coil wound in the threads was enclosed in a silver chloride sleeve (0.075–0.150 cm thick) with end caps. Pyrophyllite sample containers with both integral preformed gaskets and metal flow seals inserted in the depressed faces of the container were used as described earlier.¹¹

At elevated temperatures, the sample was enclosed in either a boron nitride or a pyrophyllite jacket. There was no apparent reaction between these materials and the CdS in the temperature range covered. Thin-wall (0.035-cm) titanium heater tubes were used in an arrangement similar to that previously described.¹¹ Temperature was monitored by Pt–Pt 13% Rh and Chromel–Alumel thermocouples introduced through the gaskets. The pressure effects on the emf of these couples have been reported.¹³

The electrical resistance measurements were performed in the cubic apparatus (up to 60 kbar) and in a two-stage piston-cylinder apparatus¹⁴ (up to 80 kbar).

¹³ R. E. Hanneman and H. M. Strong, *Am. Soc. Mech. Engrs. Paper 64-WA/PT-21* (1964).

¹⁴ A. A. Giardini, J. E. Tydings, and S. B. Levin, *Am. Mineralogist* **45**, 217 (1960).

⁴ A. Jayaraman, W. Klement, Jr., and G. C. Kennedy, *Phys. Rev.* **130**, 2277 (1963).

⁵ C. J. M. Rooymans, *Phys. Letters* **4**, 186 (1963).

⁶ A. N. Mariano and E. P. Warekoi, *Science* **142**, 672 (1963).

⁷ S. S. Kabalkina and Z. V. Troitskaya, *Dokl. Akad. Nauk SSSR* **151**, 1068 (1963) [English transl.: *Soviet Phys.—Doklady* **8**, 800 (1964)].

⁸ J. A. Corll (private communication), and *J. Appl. Phys.* **35**, 3032 (1964).

⁹ A. A. Giardini, E. H. Poindexter, and G. A. Samara, *Rev. Sci. Instr.* **35**, 713 (1964).

¹⁰ A. Van Valkenburg, in *High Pressure Measurement*, edited by A. A. Giardini and E. C. Lloyd (Butterworths Scientific Publications, Inc., Washington, D. C., 1963), p. 87.

¹¹ G. A. Samara, A. Henius, and A. A. Giardini, *J. Basic Eng.* **86**, 743 (1964).

¹² A. A. Giardini and G. A. Samara, *Am. Soc. Mech. Engrs. Paper 64-WA/PT-10* (1964).

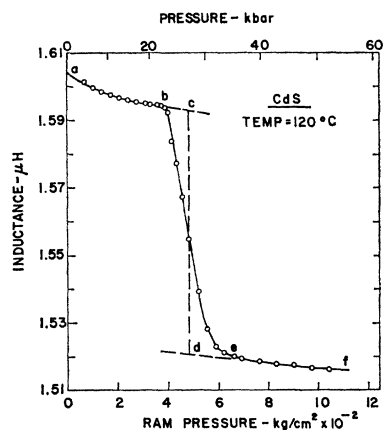


FIG. 2. Inductance of a coil wound on a threaded CdS as a function of ram pressure at 120°C. Lead inductance was 0.6125 μH .

Measurements were made on Harshaw "pure" single-crystal and compacted-powder samples both prepared in the form of thin cylindrical disks (0.30–0.45) cm diam \times (0.040–0.100) cm thick. Thin gold foil electrodes were used in contact with the large faces of the sample. There was some evidence of non-Ohmic contacts especially in the low-pressure phase. No correction for contact resistance was applied. The samples were encapsulated in silver chloride for room-temperature experiments and in boron nitride or pyrophyllite for high-temperature experiments.

Pressure was measured both by the recently developed Manganin gauge with integral calibrants¹⁵ and by multiple event resistance cells.¹¹

III. RESULTS AND DISCUSSION

a. Compressibility

Four experiments were performed at room temperature (22–25°C) and one at 120°C. Figure 1 is a typical inductance versus pressure curve and Fig. 2 is the corresponding 120°C isotherm. The large hysteresis of the transition is illustrated in Fig. 1, where the reversibility data has been corrected for the frictional hysteresis of the apparatus. Both the sluggishness and the hysteresis of the transition decrease with increasing temperature. At room temperature the transition starts at 23 ± 1 kbar and is complete by 35–37 kbar. At 120°C it started at 24 ± 1 kbar and was complete by 33–35 kbar.

In the experimental arrangement used, the coil collapses with the sample under pressure, and the inductance L is related to sample volume V by⁹

$$L \propto V^{1/3}. \quad (1)$$

The volume changes for all runs are summarized in Table I. The table lists the volume changes at various regions of the compression curve. These regions are indicated by the lower case letters in Figs. 1 and 2. The

¹⁵ G. A. Samara and A. A. Giardini, Rev. Sci. Instr. **35**, 989 (1964).

TABLE I. Summary of the compressibility data of CdS at 25°C giving the volume changes at various regions of the compression curve. The start of each region is taken as the reference volume in calculating the percent volume change for that region. The various regions are labeled by the lower case letters and are identified in Figs. 1 and 2.

Sample dimensions (cm) ^a	$-\Delta V/V$ (%) a-b (0–23 kbar)	$-\Delta V/V$ (%) c-d (Trans.)	$-\Delta V/V$ (%) b-e	$-\Delta V/V$ (%) a-f (0–55 kbar)
$l=0.634$ $d=0.635$	4.1	21.5	23.5	28.0
$l=0.635$ $d=0.635$	4.5	21.5	23.8	28.8
$l=0.755$ $d=0.622$	4.1	20.2	22.4	27.3
$l=1.263$ $d=0.901$	4.2	20.8	22.3	26.5

^a l = length; d = diameter.

volume discontinuity at the transition is calculated from the vertical drop in the inductance as indicated by the dashed lines (c)–(d).

The compression curve of CdS at 25°C is shown in Fig. 3, and the data is tabulated in Table II at 5-kbar increments. The data represent the average values of the four runs. The compression curve at 120°C is, to within $\pm 5\%$, the same as that in Fig. 3. The volume change at the transitions is higher (22 versus 21%) and the compression of the high-pressure phase slightly smaller than the corresponding changes at 25°C.

The average volume compressibility is defined by

$$K = \frac{-1}{V_0} \left(\frac{\Delta V}{\Delta p} \right)_T. \quad (2)$$

From the present data we get for the compressibilities of the two phases

$$\text{Wurtzite phase (0–23 kbar): } K = 18.2 \times 10^{-4} \text{ kbar}^{-1}$$

$$\text{Rocksalt phase (40–60 kbar): } K = 9.5 \times 10^{-4} \text{ kbar}^{-1}.$$

These values are in good agreement with the x-ray results of Kabalkina and Troitskaya.^{7,16}

For the volume discontinuity at the transition, we get an average value of 21% at 25°C. Jayaraman *et al.*,⁴ using the piston displacement technique, obtained a value of $\sim 10\%$. Very good agreement is obtained between our results and the x-ray data. Roymans⁵ gives for the lattice parameter of the rocksalt phase a value of $a = 5.30 \text{ \AA}$ and Mariano and Warekois⁶ a value of

¹⁶ S. S. Kabalkina and Z. V. Troitskaya (see Ref. 7) present two graphs for the hexagonal wurtzite phase, one showing the variation of a and c with pressure, and the other showing the unit cell volume versus pressure. The two graphs are not consistent. Their lattice parameters measured at 1 bar agree with the known parameters namely $a = 4.14 \text{ \AA}$, and $c = 6.72 \text{ \AA}$. Since there are two molecules per unit cell for the wurtzite structure, we calculate a volume of $49.8 \text{ \AA}^3/\text{molecule}$ versus a value of $57.5 \text{ \AA}^3/\text{molecule}$ reported by the above authors. It appears that they calculated their hexagonal cell volume using the formula $V = a^2c$ which gives a value of $57.5 \text{ \AA}^3/\text{molecule}$. This mistake leads to an error in their reported value for the compressibility of the low-pressure phase ($K = 15.3 \times 10^{-4} \text{ kbar}^{-1}$) and also in the calculated value for the sudden volume change at the transition (29.6%).

TABLE II. Compression of cadmium sulfide at 25°C.

P (kbar)	$-(\Delta V/V_0)$ (%)	P (kbar)	$-(\Delta V/V_0)$ (%)
0	0	35	25.70
5	1.20	40	26.40
10	2.15	45	26.95
15	3.00	50	27.40
20	3.80	55	27.85
	^a	60	28.25
25	8.50		
30	19.65		

^a Sudden volume change at transition 4.75 to 25.30% (see Fig. 3).

5.32 Å, both presumably measured just above the transition. Kabalkina and Troitskaya⁷ give a value of $a=5.27$ Å at 88.5 kbar. Accounting for the compressibility of the rocksalt phase, this corresponds to a value $a=5.34$ Å at 30 kbar. Using the average value of $a=5.32$ Å one calculates a total volume change $\Delta V/V_0$ of -24.5% . Subtracting from this the compression of the wurtzite phase, namely, 4% gives for the sudden volume change a value of 20.5% which is in excellent agreement with our value of 21% .

The agreement between the present results and the x-ray data speaks well for the inductive coil method. In the data presented, no corrections were made other than subtracting the constant inductance of the lead-in cable to the coil from the total measured inductance. This varied between 8 and 60% of the total inductance for the various runs. The principal source of error in the technique is the change in inductance caused by distortion of the coil and leads. We have reduced both of these to a minimum, and it is felt that the error so introduced is less than 5% of the volume changes.

b. Electrical Resistance

Room-temperature resistance versus pressure measurements were performed on two single crystals and

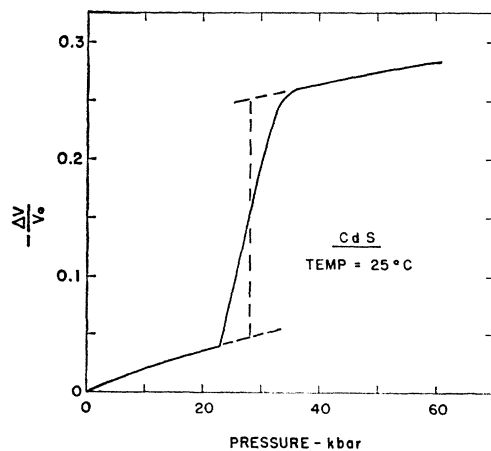


FIG. 3. Compression curve of CdS at 25°C.

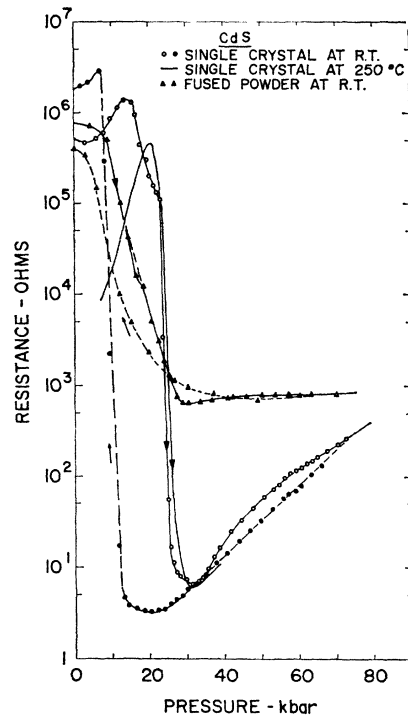


FIG. 4. Resistance-versus-pressure isotherms for CdS samples initially in the wurtzite phase. For the 25°C isotherms, initial resistivities were $\sim 5 \times 10^5 \Omega \text{ cm}$ and $\sim 1.4 \times 10^6 \Omega \text{ cm}$ for the single-crystal and fused-powder samples, respectively. For the 250°C isotherm, initial sample resistivity was $3 \times 10^7 \Omega \text{ cm}$.

one compacted powder pellet all initially in the wurtzite form. Figure 4 shows the results for one of the crystals and the powder sample. The initial resistivities were $\sim 5 \times 10^5 \Omega \text{ cm}$, and $\sim 1.4 \times 10^6 \Omega \text{ cm}$, respectively. In the low-pressure phase, the features in the resistance-versus-pressure curve for the two crystals varied somewhat, but the over-all behavior was the same. In both crystals a sharp decrease in resistance of over four orders of magnitude was observed at 23 kbar. This is the same pressure at which the transition started in the volume studies. The resistance exhibits a minimum at ≈ 31 kbar which pressure probably corresponds to the end of the transition. Above this point the resistance increases with pressure. Between 35 and 80 kbar the increase is by more than a factor of 30. The behavior is reversible with a sample hysteresis of 13 kbar for the transition.

The behavior of the powder sample was quantitatively much different; however, the qualitative features are about the same. The transition starts at a much lower pressure, but the minimum in the resistance occurs at about the same pressure as for the crystalline samples, although the resistivity is some two orders of magnitude higher. Beyond the minimum the resistance rises only slightly with pressure.

Two resistance experiments were performed at elevated temperature and pressure with single crystals.

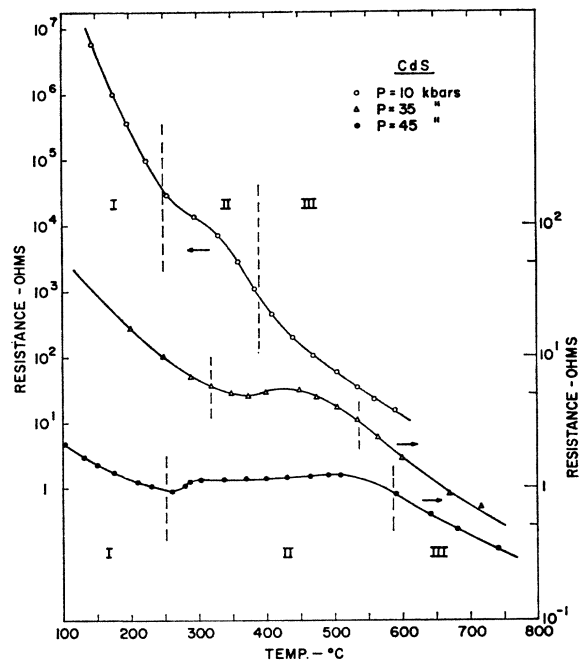


FIG. 5. Resistance-versus-temperature isobars for the wurtzite and rocksalt phases of CdS. The isobars are from different experiments.

The purpose was to study the nature of the conductivity of the two phases. Isobars of resistance versus temperature (up to $\sim 700^\circ\text{C}$) were measured at two pressures below and two pressures above the transition. Because of the high temperatures involved, no pressure calibration cells were used in these two experiments. It is not known exactly how much temperature cycling up to these temperatures influences the pressure calibration in view of the fact that pyrophyllite undergoes a transformation (to coesite and kyanite) around 600°C at elevated pressures. In any case, the uncertainty in the pressure introduced by assuming that the room-temperature calibration holds is not important for the purpose of these two experiments. It may be important in determining the effect of temperature on the transition pressure.

Figure 5 shows isobars of the resistance-versus-temperature behavior in the low- and high-pressure phases. The three isobars are from different samples. Both phases exhibit semiconducting behavior.

The change of resistance with pressure at 250°C is shown by the solid curve in Fig. 4. There is a sharp maximum at 20 kbar. The start of the transition is not as well defined as for the room-temperature isotherm, but it appears to be close to the same pressure. The minima in the resistance of the two isotherms also occur at about the same pressure.

The electronic conductivity σ of semiconductors is generally controlled by the production of charge carriers and varies with temperature according to the

relationship

$$\sigma = A e^{-E/kT}, \quad (3)$$

where A is a constant (which lumps together the mobility and effective mass of the charge carriers and the density of states) and kT has the usual meaning. In the extrinsic range, E is the ionization (or activation) energy of the impurity, while in the intrinsic range, $E = \frac{1}{2}E_g$, where E_g is the band gap.

Cadmium sulfide is a wide-band-gap semiconductor. Its energy gap, determined by optical techniques, is ≈ 2.5 eV at atmospheric pressure. With such a large gap, any measurable conductivity at moderately low temperatures is due to carriers furnished by ionized impurities or imperfections (e.g., vacancies). In CdS the carriers are always found to be electrons at atmospheric pressure. This is attributed to a much higher activation energy for p -type impurities ($E > 0.5$ eV) than for n -type impurities.¹⁷ Donor levels are usually located < 0.03 eV below the conduction band,¹⁷ and thus donors should be completely ionized at room temperature. The high resistivity ($\rho > 10^5 \Omega \text{ cm}$) of the samples used in the present study is due to both a high degree of compensation of donors and acceptors and the purity of the samples.

The temperature dependence of the electrical resistance of CdS exhibits the three distinct temperature regions (see Fig. 5) typical of extrinsic semiconductors. From the data in Fig. 5 we find that at 10 kbar the activation energy in region I is $E = 0.9$ eV. It increases to 0.95 eV at 18.5 kbar, and $\Delta E/\Delta p = 6 \times 10^{-3}$ eV/kbar.

In region III (intrinsic range), the data in Fig. 5 yield for the band gap a value $E_g = 2.3$ eV at 10 kbar. At 18.5 kbar we get $E_g = 2.7$ eV. These values compare favorably with the atmospheric value of ≈ 2.5 eV obtained from spectroscopic data. The observed increase in E_g with pressure is in qualitative agreement with the optical measurements which give $dE_g/dp = 3.3 \times 10^{-3}$ eV/kbar.¹ The much larger increase observed in the present work may be due in part to change in contact resistance.

For the high-pressure rocksalt phase, the two isobars in Fig. 5 are from different samples. The activation energies in region I are 0.2 eV for the 35-kbar isobar and 0.1 eV for the 45-kbar isobar. From the data in region III we estimate an energy gap of ≈ 1.3 eV for the rocksalt phase. The optical results give $E_g \approx 1.7$ eV.¹ A contributing factor for this discrepancy is the fact that the optical gap was measured at an absorption coefficient of 30 cm^{-1} instead of zero. The optical gap would then be expected to be larger than that measured by electrical resistivity. The discrepancy may also be due partly to the fact that the sample is polycrystalline in this phase and thus the conductivity is not truly intrinsic and partly to the influence on σ of changes in mobility which may not be negligible for the conditions

¹⁷ D. G. Thomas, in *Semiconductors*, edited by N. B. Hannay, (Reinhold Publishing Corporation, New York, 1959), p. 290.

in this region. Equation (3) assumes that the mobility is constant. In region II of the isobars in Fig. 5 carrier mobility is the controlling factor in the conduction mechanism.

The increase in the resistance of both the wurtzite and rocksalt phases of CdS with pressure at constant temperature deserves some comment. Pressure affects the conductivity through changes in both the concentration and mobilities of the charge carriers. For an extrinsic semiconductor the term A in Eq. (3) is given by:

$$A = (2N)^{1/2} (2\pi m^* kT / h^2)^{3/4} \mu |e|, \quad (4)$$

where N is the concentration of impurity atoms, m^* is the effective mass, μ is the mobility of the charge carrier, h is Planck's constant, and e is the electronic charge. Thus from Eqs. (3) and (4), we see that the change of σ with pressure is dependent on the variations of m^* , μ , and E .

The fractional change in m^* with pressure is approximately the same as the fractional change in $E_g(m^* \sim E_g)$.¹⁸ It is of the order of $+1 \times 10^{-3}$ kbar⁻¹ for the wurtzite phase and -3×10^{-4} kbar⁻¹ for the rocksalt phase.¹ The functionality of μ depends on the scattering mechanism involved (e.g., thermal and ionized impurity scattering) and is quite complicated.¹⁹ However, it can be argued¹⁸ that the fractional change in μ is also of the order 10^{-3} kbar⁻¹. These variations in m^* and μ are too small to account for the observed changes in the resistance, and thus the predominant effect must be due to E . E appears in the exponential term and σ is very sensitive to small changes in it. Neglecting the pressure dependence of m^* and μ one can, on the basis of Eq. (3), write

$$\frac{\partial \ln \rho}{\partial p} = \frac{1}{kT} \left(\frac{\partial E}{\partial p} \right), \quad (5)$$

where $\rho (=1/\sigma)$ is the resistivity.

The validity of Eq. (5) in the wurtzite phase can be tested. From the 250°C isotherm in Fig. 5 (in the range 10–20 kbar), $\partial \ln \rho / \partial p = 0.15$ kbar⁻¹. Over this range $(\partial E / \partial p) = 6 \times 10^{-3}$ eV/kbar,²⁰ and therefore, $(1/kT) \times (\partial E / \partial p) = 0.14$ kbar⁻¹. The agreement is quite good.

No measurements were made to determine $(\partial E / \partial p)$ for the rocksalt phase, but from the 25°C single-crystal data in Fig. 4 and Eq. (5) we estimate a value of $\approx 1 \times 10^{-3}$ eV/kbar. However, Eq. (5) may not be as valid here as for the wurtzite phase in view of the fact that the conductivity of the rocksalt phase is orders of magnitude higher than that of the wurtzite phase, and

¹⁸ W. Paul and D. M. Warschauer, in *Solids Under Pressure*, edited by W. Paul and D. M. Warschauer (McGraw-Hill Book Company, Inc., New York, 1964), p. 179.

¹⁹ F. J. Blatt, in *Solid State Physics*, edited by S. Seitz and D. Turnbull (Academic Press Inc., New York, 1957), Vol. 4, p. 199.

²⁰ These values of $\partial \ln \rho / \partial p$ and $(\partial E / \partial p)$ were obtained for crystals cut from the same ingot.

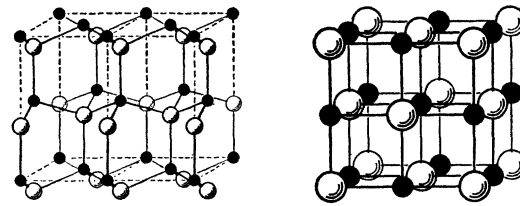


Fig. 6. The arrangement of Cd atoms (solid circles) and S atoms (open circles) in the hexagonal wurtzite (left) and cubic rocksalt (right) forms of CdS.

therefore, changes in mobility with pressure may not be negligible in this case.

c. The Transition

A look at the nature of the wurtzite-rocksalt transformation in CdS is of interest. The spatial arrangements of the atoms in these two structures are shown in Fig. 6. In the wurtzite form each cadmium atom is tetrahedrally surrounded by four sulfur atoms and vice versa. This is the same atomic arrangement as in the highly covalent group IV elements and III-V compounds which crystallize in the diamond and zincblende structures, respectively. In CdS as well as in the other II-VI compounds, the bonding, although more ionic,^{21,22} retains much of the properties of the covalent bond which is characterized by high strength and stability. The latter account for the relative low compressibilities of these elements and compounds despite the fact that their structures are loosely packed.²³ On the basis of their low compressibilities and loose packing, phase transformations with large volume changes can be expected to occur in these materials at high enough pressures. Such is indeed the case.^{2,3}

In the rocksalt structure each cadmium atom is surrounded by six sulfur atoms. This atomic configuration is prevalent in the more ionic-bonded compounds such as PbS and KCl. That the rocksalt form of CdS may be highly ionic is supported by comparing the sum of the ionic radii with the observed interatomic distance of 2.73 Å.²⁴ The ionic radii are²⁵ Cd⁺⁺=0.97 Å and S⁻⁻=1.84 Å, giving a sum of 2.81 Å. On the other hand, the covalent radii are Cd=1.48 Å and S=1.04 Å for a sum of 2.52 Å. It is also interesting to note that the rocksalt phase of CdS is fairly compressible. Using

²¹ L. Pauling, *The Nature of the Chemical Bond* (Cornell University Press, Ithaca, New York, 1960), 3rd ed., p. 90.

²² On the basis of Pauling's electronegativity scale, it is estimated that CdS has $\sim 15\%$ ionic character. The actual value is probably more like 50% as in ZnS (see Ref. 21). On the basis of measured electroelastic properties, D. Berlincourt, H. Jaffe, and L. R. Shiozawa [Phys. Rev. **129**, 1009 (1963)] estimate that the charge on the Cd atoms in CdS is +0.84 e.

²³ At 50 kbar $\Delta V / V_0$ is -5% for Ge and -4.9% for ZnS. By way of comparison, at the same pressure, $\Delta V / V_0$ is -13% for NaCl and -9.9% (including 2% at transition) for PbS.

²⁴ The unit cell volume of the rocksalt phase extrapolated back to atmospheric pressure gives $a^3 = 5.50$ Å. J. A. Corll (see Ref. 8) reports a value $a_0 = 5.464 \pm 0.012$ Å for material recovered in the rocksalt phase at atmospheric pressure and temperature.

See Ref. 21, p. 514.

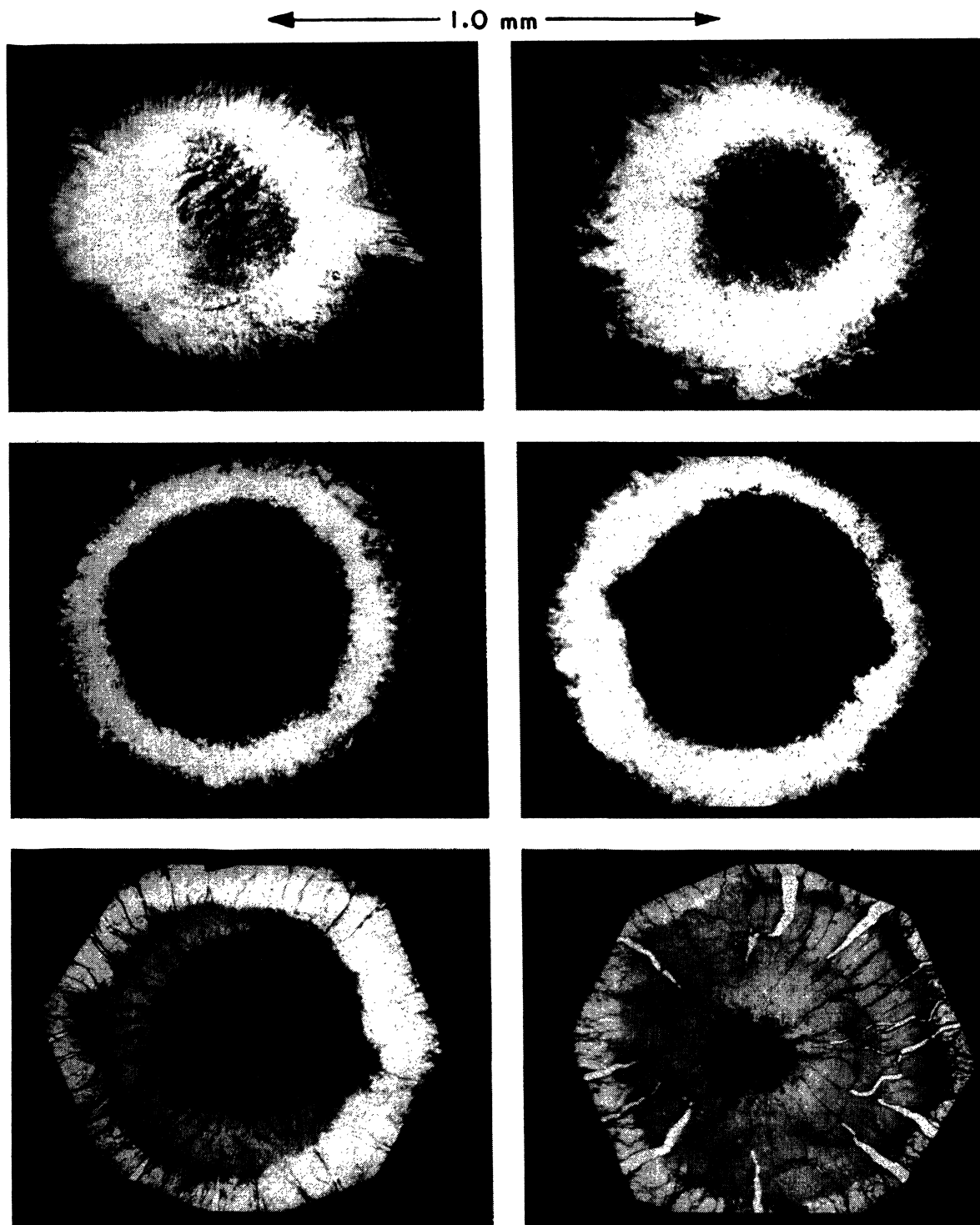


FIG. 7. A series of photographs showing the progress of the forward and reverse transformation in CdS. The different views are described in the text.

Corll's⁸ value of $a_0=5.46$ Å (atmospheric) and a calculated value of $a=5.30$ Å at 50 kbar, one gets for the rocksalt phase a total compression $\Delta V/V_0$ of -8.6% at 50 kbars.

The transformation between the two structures in Fig. 6 is a reconstructive one in which Cd-S bonds must break and reform in order to effect the structural change. The likely mechanism is as follows: When the critical pressure is reached, the wurtzite structure becomes unstable. The rocksalt phase then starts to form. Formation of the latter phase is a kinetic process, the controlling steps being either the rate of formation of nucleation sites or the rate of crystal growth. It is almost certain that no bulk diffusion is involved. This is supported by the fact that shock wave experiments²⁶ have shown that the transformation is complete in a time of the order of a microsecond, a time scale much too short for bulk diffusion to take place.

We have examined the progress of the transition visually under high magnification, and the observations appear to be consistent with the above remarks. A high-pressure cell of the type described by Van Valkenburg¹⁰ was mounted in an optical microscope, and photographs were taken at various stages of the transformation. A series of photographs showing the progress of the wurtzite \rightarrow rocksalt and rocksalt \rightarrow zincblende transitions are shown in Fig. 7. Thin wurtzite flakes were used.

The transition starts at the center of the sample, this being the region of highest pressure between the diamond anvils. At the first indication of the start of the transformation, microscopic brownish areas appear in the bright yellow wurtzite phase. These are grainy and appear to be a mixture of crystallites of both wurtzite and rocksalt phases. With increased pressure these areas become larger and join, and small crystals of the new phase become quite apparent. This is shown in the upper left-hand picture in Fig. 7. The white outer ring is the untransformed wurtzite phase. The center part is a mixture of the two phases and is brown in color.

At still higher pressure the transition areas expand and coalesce, and homogeneous regions of the new phase begin to appear. The progress of this process is shown in sequence in the upper right-hand and center left-hand photos in Fig. 7. The right center photo was taken at the end of the transformation. The center part of the photo is the rocksalt phase. It is deep red in color. The outer white ring (actually yellow) is the untransformed wurtzite phase. The two phases are separated by a ring of mixed phases.

Upon the release of the pressure the rocksalt phase transforms mostly into the zincblende structure rather than reverting completely to the wurtzite form. This is

clearly exhibited by color changes and is illustrated by the two bottom photographs in Fig. 7.²⁷ The center region is again rocksalt phase. The outer ring is the new zincblende phase. It has a bright orange color. The outermost ring is the original wurtzite form. At low enough pressure all the rocksalt phase transforms.

d. Transition Pressure

In all our room-temperature experiments on wurtzite single crystals, the transition in CdS started at a lower applied load than the Bi_{T-II} transition. In many of these experiments the two transitions were monitored simultaneously. The transition starts at 23 ± 1 kbar at 25°C. For the large samples used in the compressibility studies the transition is complete by 35–37 kbar. For the much smaller crystals used in the resistance measurement, the minimum in the resistance curve, which probably corresponds to the end of the transition, occurs at 30–31 kbar. A part of this observed sluggishness is inherent in the material and part is associated with the "cave" effect described previously.^{11,15}

The transition has a hysteresis of $\simeq 12$ kbar (corrected for the hysteresis of the apparatus). This was measured midway through the transition and not as the difference between the starts of the forward and reverse transitions, since the start of the latter was not as sharp and well defined as the start of the forward transition.

The transition pressure is weakly dependent on temperature. Four experiments, two volumetric and two electrical resistance, were performed at elevated temperatures in order to determine the slope of the phase boundary. No pressure calibration cells were used in these experiments, and it was assumed that the room-temperature pressure calibration holds. The volumetric experiments, which were performed below 200°C, exhibited an increase of the transition pressure of $\sim 1.2 \times 10^{-2}$ kbar/°C. The resistance experiments, on the other hand, exhibited a comparable decrease of the transition pressure with temperature. However, in these experiments resistance-versus-temperature isobars were measured up to over 600°C before going through the transition, and, therefore, there may be some uncertainty in the pressure calibration, as mentioned earlier.

ACKNOWLEDGMENTS

The authors express their appreciation to R. Baughman of Sandia Laboratory for providing some of the samples used in this work and to E. H. Poindexter, J. A. Corll, and J. D. Barnett for many helpful discussions. Special thanks are also extended to F. J. Becker for his excellent support in component fabrication and to G. E. Tomes for his assistance in performing some of the experiments.

²⁶ J. D. Kennedy and W. B. Benedick, private communication and work to be published.

²⁷ Cracking develops in the thin sample between the diamond anvils upon lowering the pressure.

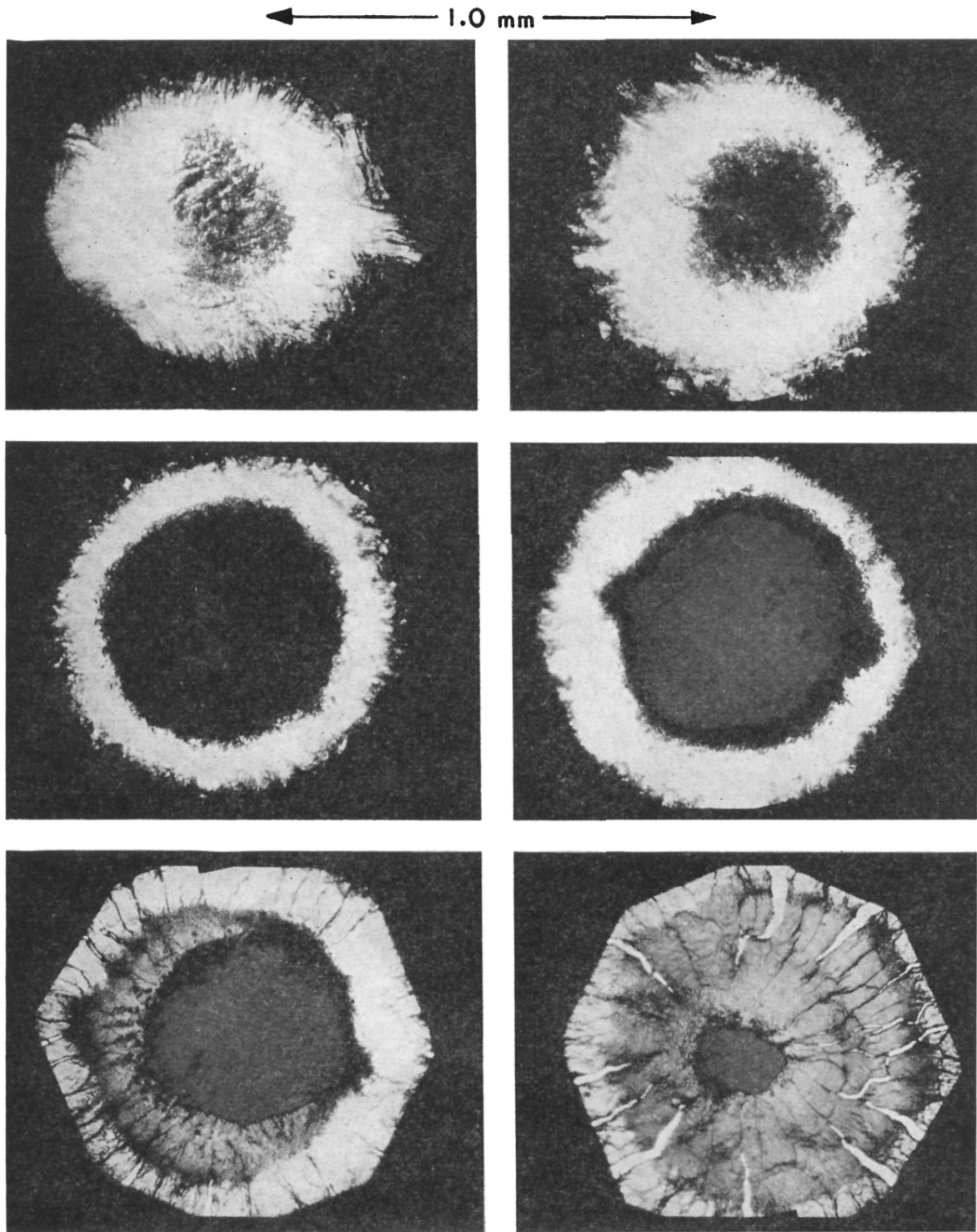


FIG. 7. A series of photographs showing the progress of the forward and reverse transformation in CdS. The different views are described in the text.